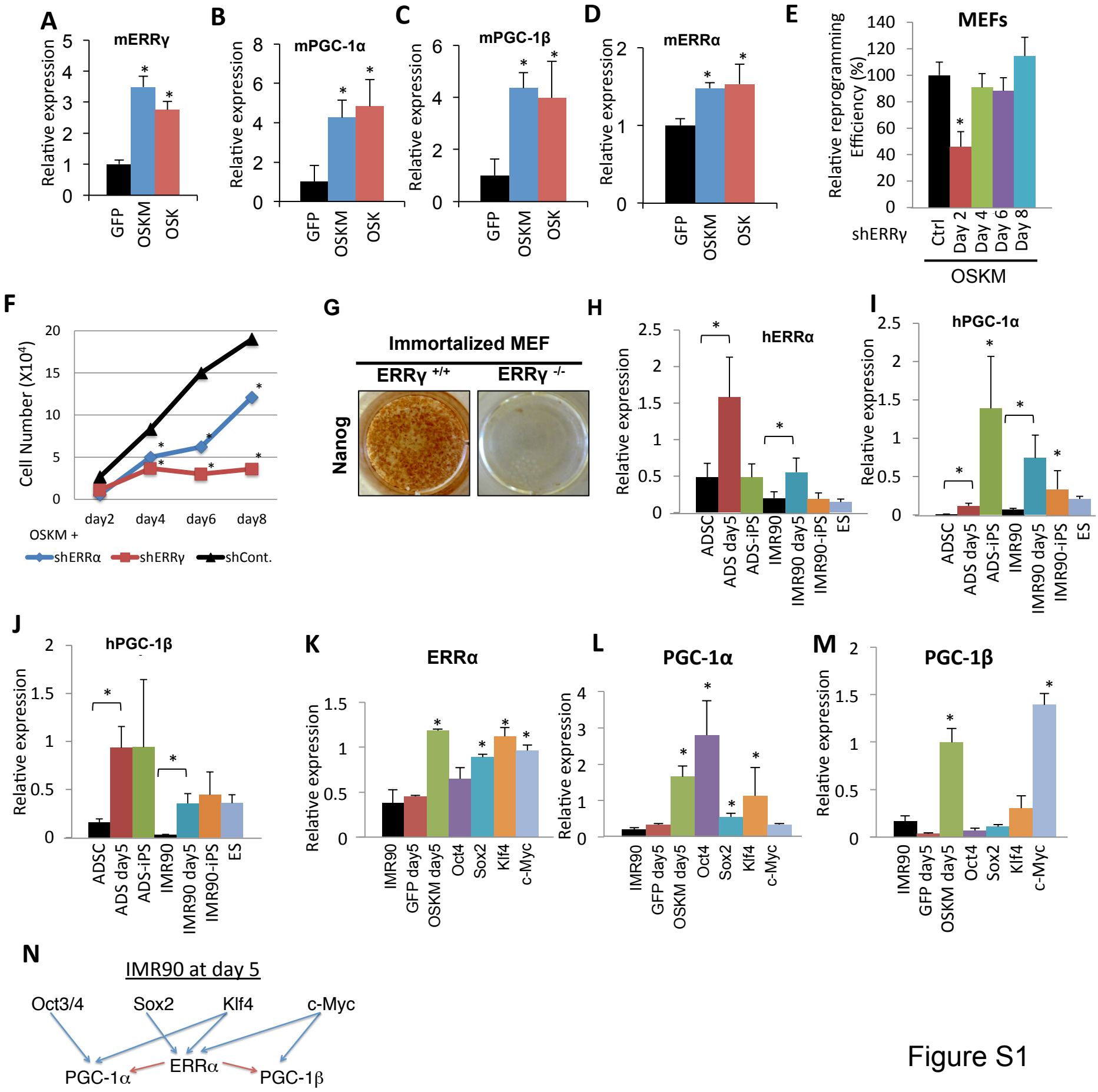
A
mERRγ
Relative expression
GFP
OSKM
OSK
B
mPGC-1α
C
mPGC-1β
D
mERRα
E
MEFs
Relative reprogramming Efficiency (%)
shERRγ
Ctrl
Day 2
Day 4
Day 6
Day 8
OSKM
F
Cell Number (X10⁴)
day2
day4
day6
day8
OSKM +
shERRα
shERRγ
shCont.
G
Immortalized MEF
ERRγ +/+
ERRγ -/-
Nanog
H
hERRα
ADSC
ADS day5
ADS-iPS
IMR90
IMR90 day5
IMR90-iPS
ES
I
hPGC-1α
J
hPGC-1β
K
ERRα
IMR90
GFP day5
OSKM day5
Oct4
Sox2
Klf4
c-Myc
L
PGC-1α
M
PGC-1β
N
IMR90 at day 5
Oct3/4
Sox2
Klf4
c-Myc
ERRα
PGC-1α
PGC-1β

Figure S1

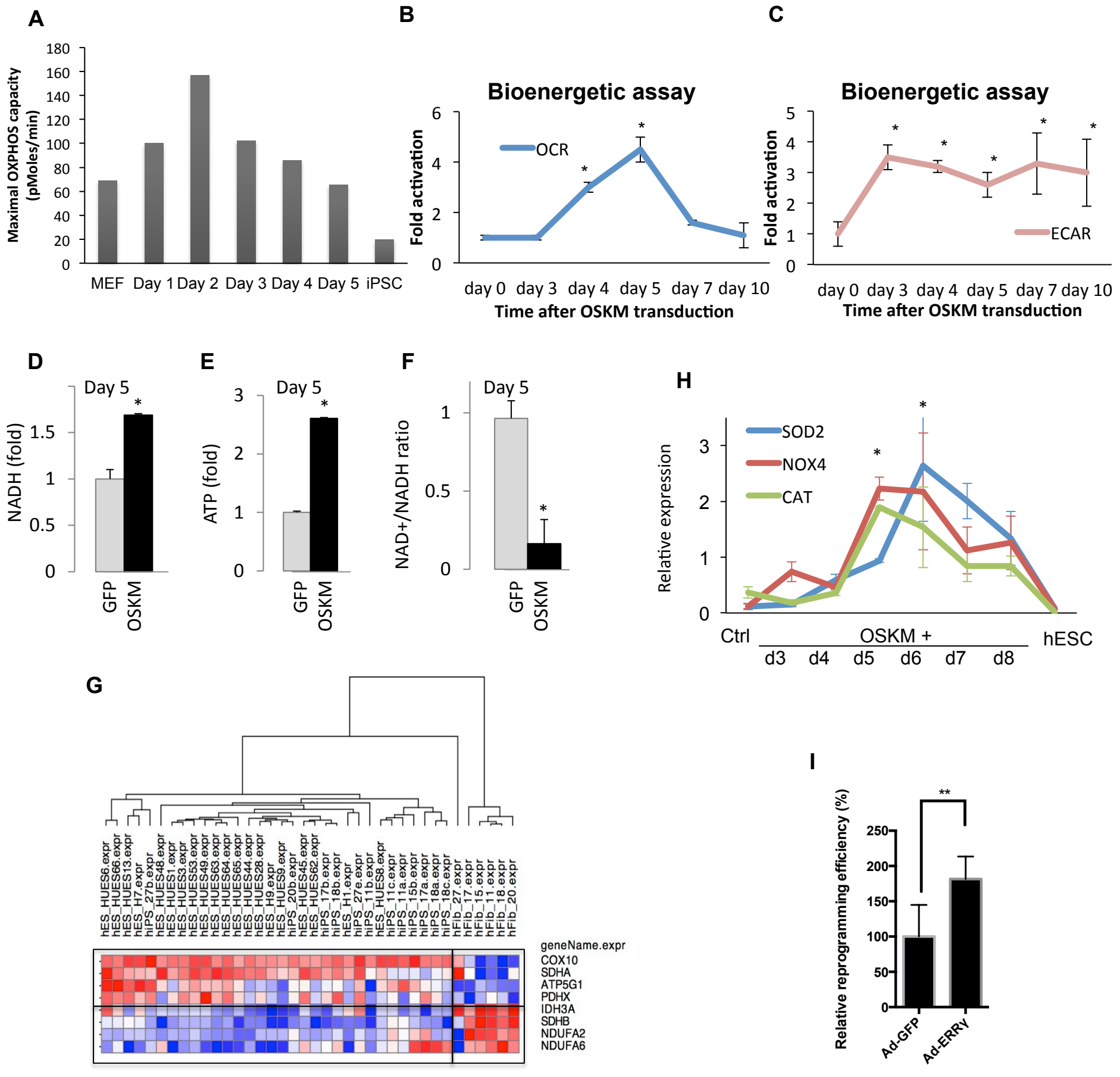
A
Maximal OXPHOS capacity (pMoles/min)
180
160
140
120
100
80
60
40
20
0
MEF Day 1 Day 2 Day 3 Day 4 Day 5 iPSC
B
Bioenergetic assay
Fold activation
6
4
2
0
OCR
day 0 day 3 day 4 day 5 day 7 day 10
Time after OSKM transduction
C
Bioenergetic assay
Fold activation
5
4
3
2
1
0
ECAR
day 0 day 3 day 4 day 5 day 7 day 10
Time after OSKM transduction
D
Day 5
NADH (fold)
1.5
1
0.5
0
GFP
OSKM
E
Day 5
ATP (fold)
3
2
1
0
GFP
OSKM
F
Day 5
NAD+/NADH ratio
1
0.5
0
GFP
OSKM
H
Relative expression
3
2
1
0
SOD2
NOX4
CAT
Ctrl
OSKM +
hESC
d3 d4 d5 d6 d7 d8
G
hES_HUES6.expr
hES_HUES66.expr
hES_HUES13.expr
hES_H7.expr
hiPS_27b.expr
hES_HUES48.expr
hES_HUES1.expr
hES_HUES3.expr
hES_HUES53.expr
hES_HUES49.expr
hES_HUES63.expr
hES_HUES64.expr
hES_HUES65.expr
hES_HUES44.expr
hES_HUES28.expr
hES_H9.expr
hES_HUES9.expr
hiPS_20b.expr
hES_HUES45.expr
hES_HUES62.expr
hiPS_17b.expr
hiPS_18b.expr
hES_H1.expr
hiPS_27e.expr
hiPS_11b.expr
hES_HUES8.expr
hiPS_11c.expr
hiPS_11a.expr
hiPS_15b.expr
hiPS_17a.expr
hiPS_18a.expr
hiPS_18c.expr
hFib_27.expr
hFib_17.expr
hFib_15.expr
hFib_11.expr
hFib_18.expr
hFib_20.expr
geneName.expr
COX10
SDHA
ATP5G1
PDHX
IDH3A
SDHB
NDUFA2
NDUFA6
I
Relative reprogramming efficiency (%)
250
200
150
100
50
0
**
Ad-GFP
Ad-ERRγ

Figure S2

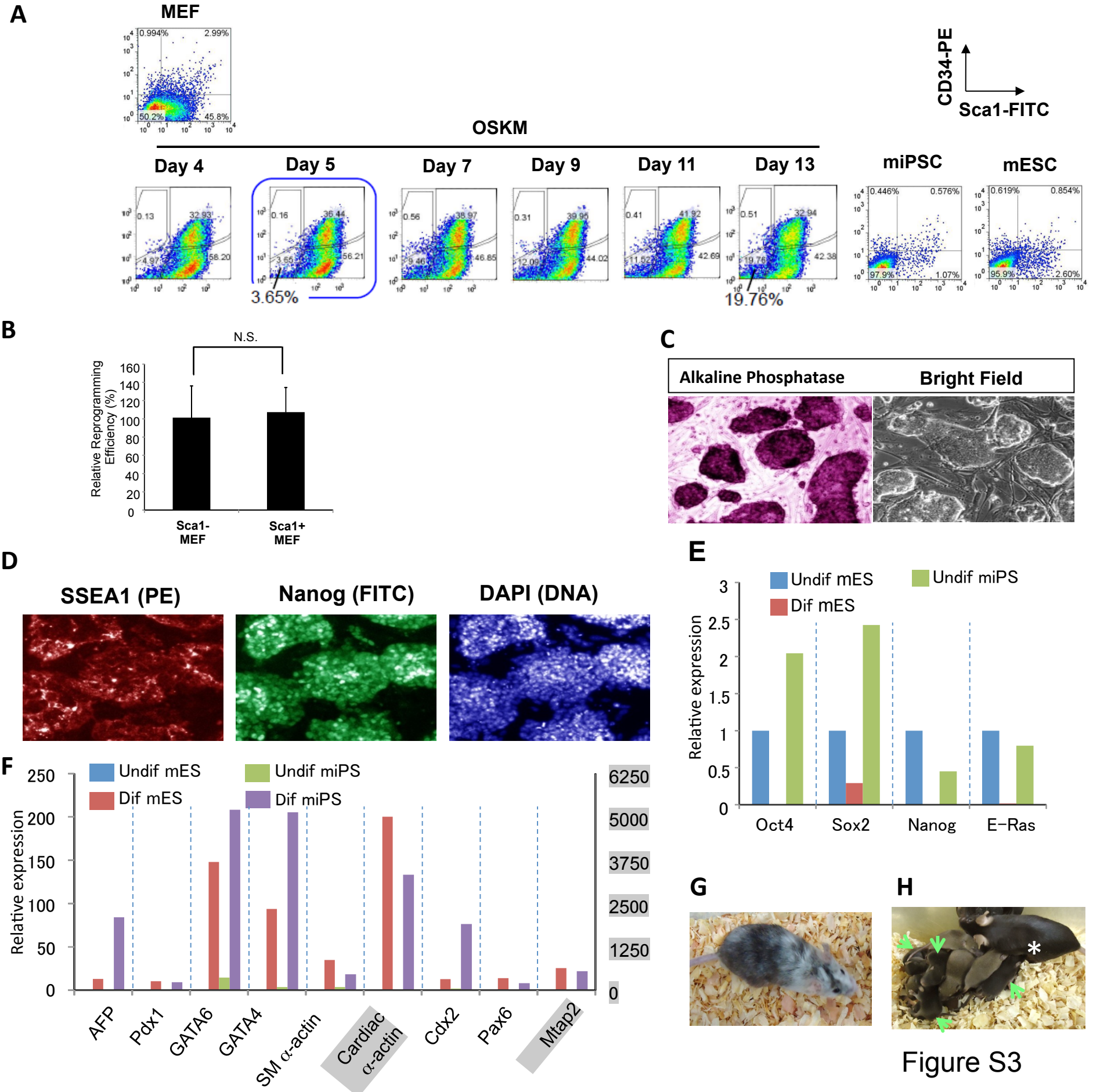
A
MEF
0.994%
2.99%
50.2%
45.8%
CD34-PE
Sca1-FITC
OSKM
Day 4
Day 5
Day 7
Day 9
Day 11
Day 13
miPSC
mESC
0.13
32.93
4.97
58.20
0.16
36.44
3.65%
56.21
0.56
38.97
9.46
46.85
0.31
39.95
12.09
44.02
0.41
41.92
11.52
42.69
0.51
32.94
19.76%
42.38
0.446%
0.576%
97.9%
1.07%
0.619%
0.854%
95.9%
2.60%
B
N.S.
Relative Reprogramming Efficiency (%)
160
140
120
100
80
60
40
20
0
Sca1-MEF
Sca1+MEF
C
Alkaline Phosphatase
Bright Field
D
SSEA1 (PE)
Nanog (FITC)
DAPI (DNA)
E
Undif mES
Undif miPS
Dif mES
Relative expression
3
2.5
2
1.5
1
0.5
0
Oct4
Sox2
Nanog
E-Ras
F
Undif mES
Undif miPS
Dif mES
Dif miPS
Relative expression
250
200
150
100
50
0
6250
5000
3750
2500
1250
0
AFP
Pdx1
GATA6
GATA4
SM α-actin
Cardiac α-actin
Cdx2
Pax6
Mtap2
G
H
*

Figure S3

**A**

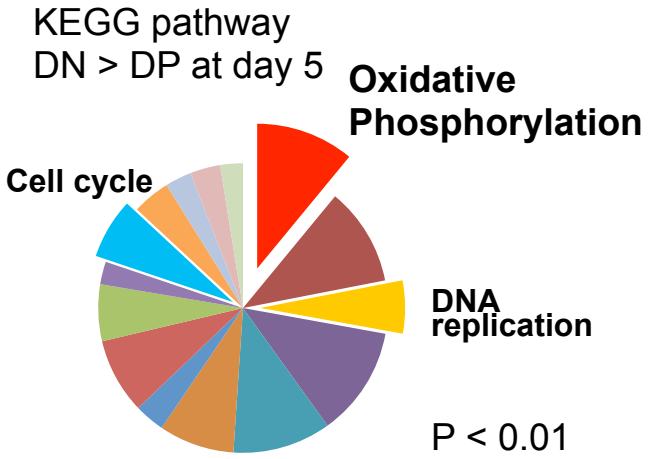


**B**

| GO term | p value |
|---|---|
| mmu00190:Oxidative phosphorylation | 1.70E-09 |
| mmu00230:Purine metabolism | 1.75E-04 |
| mmu00240:Pyrimidine metabolism | 1.81E-04 |
| mmu00670:One carbon pool by folate | 7.12E-04 |
| mmu04110:Cell cycle | 1.17E-03 |
| mmu00260:Glycine, serine and threonine metabolism | 3.75E-03 |
| mmu00290:Valine, leucine and isoleucine biosynthesis | 1.37E-03 |
| mmu04115:p53 signaling pathway | 4.75E-03 |
| mmu00270:Cysteine and methionine metabolism | 7.25E-03 |

**C**

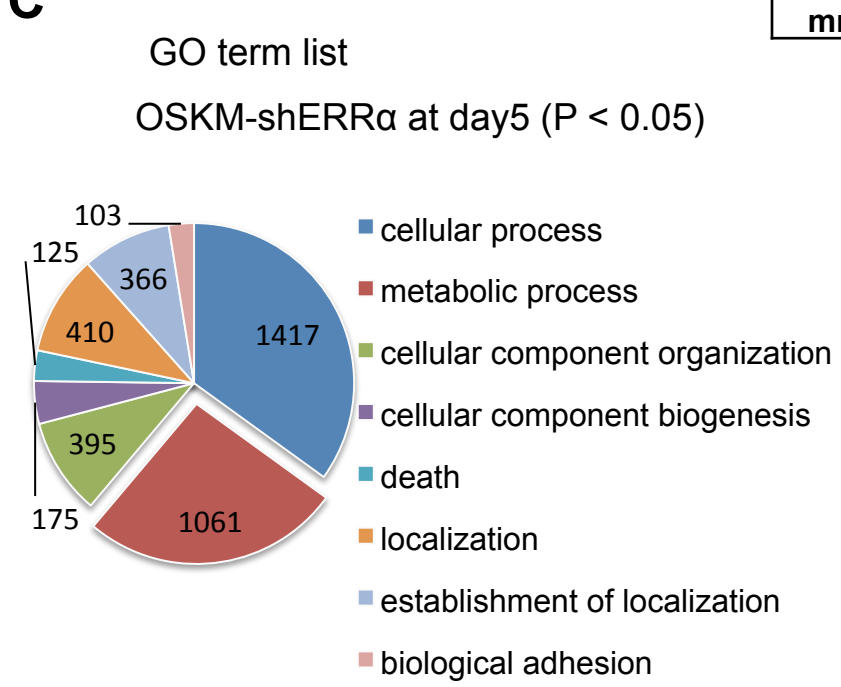


Figure S4

**Supplemental Data**

**Supplemental Figure Legends**

**Figure S1**, **related to Figure 1. ERRs and PGC1α/β are direct targets of reprogramming factors during early reprogramming.**

**A-D**. Mouse ERRα/γ and PGC1α/β are activated in retroviral reprogramming MEFs at day 3, shown by qPCR results (n=3, *p<0.01, error bars show s.e.m.).

**E**. Depleting ERRγ in retroviral reprogramming MEFs after day 4 does not influence reprogramming efficiency (n=3, error bars show s.d.).

**F**. Reprogramming cells with ERRα or ERRγ depletion by lentiviral shRNA show a reduced proliferation rate.

**G**. Nanog staining of immortalized MEFs from wild-type ($ERR\gamma^{+/+}$) or ERRγ knockout ($ERR\gamma^{-/-}$) embryos after retroviral OSKM reprogramming.

**H-J**. Human ERRα and PGC1α/β are up-regulated in retroviral reprogramming IMR90 cells at day 5, but not in adipose stem cells (ADSCs), IMR90, or pluripotent stem cells (n=3, *p<0.01, error bars show s.e.m.).

**K-M.** qPCR showing relative expression of ERRα, PGC-1α and PGC-1β in single factor infected cells (n=3, error bars show s.e.m.).

**N.** Schematic representation of ERRα, PGC-1α and PGC-1β induction by Oct3/4, Sox2, Klf4 or c-Myc.

**Figure S2, related to Figure 2. Changes in metabolic activity and ROS genes during reprogramming.**

**A**. Kinetics of maximal OXPHOS capacity in doxycycline-inducible reprogramming MEFs. Reprogramming cells at days 2 to 5 have higher OXPHOS capacity than MEFs and iPSCs.

**B-C.** Time course measurements of OCR (B) and ECAR (C) in retroviral reprogramming IMR90 cells show an up-regulated metabolic profile in early reprogramming human fibroblasts.

**D-F.** In early retroviral reprogramming of IMR90 cells, NADH, ATP and NAD+/NADH levels are changed (n=5, error bars show s.d. *p<0.01).

**G.** Metabolic genes listed in Figure 2D show a similar expression pattern between various human ES and iPS lines, in contrast to fibroblast (hFib) lines.

**H.** The dynamic expression pattern of ROS genes SOD2, NOX4 and CAT during retroviral reprogramming of IMR90 cells (n=3, error bars show s.e.m. *p<0.01).

I. Relative reprogramming efficiencies of doxycycline-inducible reprogramming MEFs with and without ERRγ over expression (Ad-ERRγ and Ad-GFP, respectively). Reprogramming efficiency based on alkaline phosphatase staining at day 21 (n=6, error bars show s.d. **p<0.01).

**Figure S3, related to Figure 3. Pluripotency assays and germline transmission of iPSCs from DN population**

**A.** Flow cytometry analysis of Sca1 and CD34 expression in WT MEFs, retroviral OSKM-infected MEFs, iPSCs and ESCs.

**B.** $Sca1^-$MEFs have similar reprogramming efficiencies to $Sca1^+$ MEFs. (n=6, error bars show s.d.)

**C.** Alkaline phosphatase staining and phase contrast image of iPSCs from DN population.

**D.** Immunofluorescence of SSEA1 (PE), Nanog (FITC) and DNA (DAPI) in iPSCs originating from $Sca1^{-}CD34^{-}$ cells.

**E, F.** q-PCR analysis of pluripotent marker genes (E) and differentiation marker genes (F) in undifferentiated and differentiated mouse ESCs and iPSCs. The scale for Cardiac a-actin and Mtap2 correspond with y-axis shaded in gray on the right.

**G**. Adult chimeric mouse obtained from an iPSC line derived from DN cell population sorted 5 days after OSKM infection.

**H**. Offspring of chimera crossed with a C56BL/6N female (asterisk) showing pups with black coats (green arrows) originating from iPSC cells.

**Figure S4, related to Figure 4. ERRα depletion affects OXPHOS burst during reprogramming.**

**A, B.** KEGG pathway analysis reveals a panel of OXPHOS related genes in DN population at 5 days after infection, suggesting up-regulation of ERRγ in bona fide reprogramming cells induce the transcription of OXPHOS program. Gene selection was based on a Bonferroni error threshold of $\alpha_{Bonf} = 0.01$.

**C.** GO analysis shows that ERRα depletion in IMR90 cells induces widespread changes of genes involved in metabolic processes.

## Supplemental Experimental Procedures

### Reprogramming

Mouse reprogramming was performed as previously described, with modifications (Kawamura et al., 2009; Sugii et al., 2010; Takahashi and Yamanaka, 2006; Yu et al., 2007). For retroviral reprogramming, pMX-based retroviral vectors harboring each of the mouse reprogramming genes (c-Myc, Klf4, Oct4, or Sox2; Addgene) were transfected along with gag/pol and VSV-G envelope genes into HEK293T cells using Lipofectamine (Invitrogen). For lentivirus production, tet-inducible lentiviral vectors containing OSKM (Wei et al., 2009) were transfected together with pspax2 and pMD2.G (Addgene). Two days after transfection, supernatants containing viruses were collected and filtered through a 0.45-μm filter. For retroviral reprogramming, a total of $1x10^4$ MEFs (passages 2–4) were infected with retroviral mixtures in 12-well plates (day 0). One well was used to quantify cell numbers for each group. Control cells were transduced with GFP retrovirus alone to determine infection efficiencies. On day 2, one-fifth of the cells were passaged onto gelatin-coated plates with MEF feeder layers (Millipore) and cultured in Knockout (KO)-DMEM containing L-glutamine (2 mM), nucleosides (1x), NEAA (non-essential amino acid; 1x), β-mercaptoethanol (1x), and LIF (1,000 units/mL), with 15% KSR (Millipore or Invitrogen). Media was changed every other day. On days 7–10, cells were either immunostained for assessing efficiencies or derived into individual colonies for downstream analyses.

For reprogramming of IMR90 fibroblasts, cells were infected with the combination of human reprogramming retroviruses (c-Myc, Klf4, Oct4, or Sox2 in pMXs; Addgene) that had been produced in 293T cells cotransfected with gag/pol and VSV-G as described

above. EGFP retrovirus was included at 1/40 volume as internal controls for transduction efficiencies. One well from each group was reserved for quantifying cell numbers. On day 2, cells were passaged onto 12-well plates containing MEF feeder cells (for generating iPSCs) or onto 6-cm dishes without MEFs (for collecting mRNAs at day 5). Cells were cultured in KO-DMEM plus 20% KSR supplemented with β-mercaptoethanol (0.1%), NEAA (1x), Glutamax (1%), and 10 ng/mL FGF2. Media was changed every day. Reprogramming of MEFs using an inducible lentiviral system was performed as previously described (Wei et al., 2009). Doxycyline-inducible MEFs were isolated from Gt(ROSA)26Sor$^{tm1(rtTA*M2)Jae}$ Col1a1tm4$^{(tetO-Pou5f1,-Sox2,-Klf4,-Myc)Jae}$/J mice (Jackson Labs) and reprogramming was performed as previously described (Carey et al., 2010). For transient overexpression of ERRγ, doxycycline-inducible MEFs, seeded at the density of 10,000 cells per well, were treated with doxycycline (2mg/ml), followed one day later by adenoviruses overexpressing eGFP or ERRγ under the control of CMV promoter (multiplicity of infection = 100). Reprogramming efficiency was measured by alkaline phosphatase staining 3 weeks after reprogramming. ERRγ-iKO mice were generated by crossing ERRγ$^{lox/lox}$ (generously provided by Johan Auwerx) and B6.Cg-Tg(CAG-cre/Esr1)5Amc/j (Jackson Labs, Cat. No. 004682) and ERRγ-iKO MEFs were isolated from E14.5 embryos. The ERRγ-iKO MEFs were reprogrammed using the inducible lentiviral system (Wei et al., 2009) and were treated by 4-hydroxytamoxifen (4-OHT) at final concentration 50nM from reprogramming day 0 to day 2. All procedures involving hiPS/hES cells were approved by the Embryonic Stem Cell Research Oversight Committee at the Salk Institute.

**Microarray analysis**

RNA was extracted from OSKM-induced at days 3, 4, 5, 6, 7 with shERRα and GFP-infected IMR90 cells at day 5 using RNeasy (QIAGEN). RNA was DNase (Ambion) treated, reverse transcribed to first-strand cDNA using a SuperScript II kit (Invitrogen), and then treated with RNase. Global gene expression analysis was performed as described (Narkar et al., 2011) .

**RNA-Seq library generation**

Total RNA was isolated from cell pellets treated with RNAlater using the RNA mini kit (Qiagen) and treated with DNaseI (Qiagen) for 30 min at room temperature. Sequencing libraries were prepared from 100-500ng total RNA using the TruSeq RNA Sample Preparation Kit v2 (Illumina) according to the manufacturer's protocol. Briefly, mRNA was purified, fragmented, and used for first-, then second-strand cDNA synthesis followed by adenylation of 3' ends. Samples were ligated to unique adapters and subjected to PCR amplification. Libraries were then validated using the 2100 BioAnalyzer (Agilent), normalized, and pooled for sequencing. RNA-Seq libraries prepared from two biological replicates for each experimental condition were sequenced on the Illumina HiSeq 2000 using bar-coded multiplexing and a 100bp read length.

**High-throughput sequencing and analysis**

Image analysis and base calling were performed with Illumina CASAVA-1.8.2. This yielded a median of 29.9M usable reads per sample. Short read sequences were mapped to a UCSC mm9 reference sequence using the RNA-seq aligner STAR (Dobin

et al., 2013). Known splice junctions from mm9 were supplied to the aligner and *de novo* junction discovery was also permitted. Differential gene expression analysis, statistical testing and annotation were performed using Cuffdiff 2 (Trapnell et al., 2013). Transcript expression was calculated as gene-level relative abundance in **f**ragments **p**er **k**ilobase of exon model per **m**illion mapped fragments and employed correction for transcript abundance bias (Roberts et al., 2011). RNA-Seq results for genes of interest were also explored visually using the UCSC Genome Browser.

**Gene Expression Analysis by qPCR**

Samples were run in triplicate and expression was normalized to the levels of the housekeeping controls Rplp0 (36b4) for human and mouse. Samples were analyzed by qPCR, using SYBR Green dye (Invitrogen). Endogenous versus exogenous reprogramming gene expression was performed as previously reported(Yang et al., 2006). Statistical comparisons were made using Student's t test. Error bars are mean ± SEM.

**Immunohistochemistry and Cell Staining**

Cells grown on dishes were immunostained using the VectaStain ABC kit and ImmPACT DAB substrate (Vector Lab) with rabbit anti-mouse Nanog (Calbiochem), anti-human Nanog (Abcam).

**Bioenergetic Assay**

Measurements were made with a Seahorse XF instrument. Adherent cells were seeded in 96-well Seahorse cell culture microplates at 20,000 per well 16 hours before measurement. Approximately 60 minutes prior to the assay, culture media was exchanged with a low-buffered DMEM assay media with 20mM glucose and 1mM sodium pyruvate. For measurement of maximal OXPHOS capacity, Oligomycin (final concentration 1.2μM), FCCP (final concentration 4μM), Antimycin A (final concentration 1μM) and Rotenone (final concentration 2μM) were added per manufacturer's instruction. The OCR and ECAR value were further normalized by measuring the cell number in each well using Hoechst 33342 staining followed by quantification of fluorescence at 355 excitation and 460 emission. The baseline OCR was defined by the average value for the first 4 measurements. The maximal OXPHOS capacity was defined by the difference between average OCR after addition FCCP (min 88-120) and OCR after addition of antimycin A and rotenone (min 131-163).

**shRNA knockdown**

shRNA constructs for mouse and human ERRα/γ and PGC-1α/β , as well as control shRNA, were purchased from Openbiosystems. Lentiviral shRNA were produced in 293T cells and polybrene (6μg/ml) was used in transduction. For reprogramming experiments, cells were transduced with lentiviral shRNA at day 0 of reprogramming.

**Live cell staining, alkaline phosphatase staining, and cell sorting**

Cells were incubated with culture media containing FITC-conjugated anti-Sca1 (1:50, Biolegend) and PE-conjugated anti-CD34 (1:100, Biolegend) antibodies for 30 minutes,

washed, then maintained in culture. Alkaline phosphatase staining was performed on formaldehyde-fixed cells using 4-Nitro blue tetrazolium chloride (450mg/ml) and 5-Bromo-4-chloro-3-indolyl-phosphate (175mg/ml) in NTMT solution (0.1M NaCl, 0.1M Tris PH9.5, 50mM MgCl2, and 0.1% Tween20). OSKM-infected cells were FACS sorted (FACSAria, BD Biosciences) 5 days after infection using FITC-conjugated anti-Sca1 (1:100) and PE-conjugated anti-CD34 antibodies (1:200), and subsequently cultured for iPS cell formation.

### *In vitro* differentiation

iPS cells were differentiated *in vitro* by embryoid body formation (Kawamura et al., 2009) with some modification. Briefly, hanging droplets (1500 single cells at 60 cells/μl in mouse ES cell media without LIF) were suspended on petri-dish lids for two or three days prior to suspension culture. Six days after differentiation, embryoid bodies were plated on gelatinized dishes for 1-2 weeks. Gene expression of pluripotency markers (Oct4, Sox2, Nanong, and E-Ras) and germ-layer markers (AFP, Pdx1, and GATA6 for endoderm; GATA4, SM α-actin, and Cardiac α-actin for mesoderm; Cdx2, Pax6, and Mtap2 for ectoderm) was determined by QPCR. Values were standardized to GAPDH and normalized to undifferentiated mouse ES cells.

### Blastocyst injections for chimeric mice

Mouse iPS cells (derived from C57BL/6N MEFs) were injected into BALB/c host blastocysts and transferred into 2.5 dpc ICR pseudopregnant recipient females. Chimerism was ascertained after birth by the appearance of black coat color (from iPS

cell) in albino host pups. High-contribution chimeras were crossed to C57BL/6N mice to test for germline transmission.

**NAD+/NADH assay**

Intracellular NAD+ and NADH levels were measured by NAD+/NADH Assay Kit (Abcam, San Francisco, CA) as per manufacturer's instructions. Briefly, $2\times10^5$ cells were washed with cold PBS and extracted with NADH/NAD Extraction Buffer by two freeze/thaw cycles (20 min on dry ice, then 10 min at room temperature). Total NAD (NADt) and NADH were detected in 96-well plates and color was developed and read at 450 nm. NAD/NADH Ratio is calculated as: [NADt – NADH]/NADH.

**Measurement of ATP**

Intracellular ATP was measured by ATP assay kit (Sigma-Aldrich) according to manufacturer’s directions. Briefly, $1\times10^4$ cells were washed with cold PBS and ATP extracted with ATP extraction buffer. Amounts of ATP were detected in 384-well plates and measured with a luminometer.